

Stationary Reference Bi Discharge Cell for Optical Diagnostics of a Bismuth Hall Thruster

IEPC-2005-058

*Presented at the 29th International Electric Propulsion Conference, Princeton University,
October 31 – November 4, 2005*

David B. Scharfe* and Mark A. Cappelli†
Stanford University, Stanford, CA, 94305, USA

Bismuth (Bi) has received considerable attention recently as a possible propellant for Hall thrusters. A bismuth-fueled Hall thruster would have advantages over conventional xenon thrusters in terms of efficiency, tankage fraction, and simplicity of ground testing facilities. In developing such a thruster, there is a need for non-intrusive diagnostic methods necessary to characterize operating conditions and performance. Important in these diagnostic options are laser-based methods that can be used to determine species (BiI and BiII) velocities and number densities. The development of these advanced diagnostics requires reliable reference Bi discharges, which can serve as convenient test articles that generate electronically excited neutral and ionized Bi species with a thermal energy distribution and a zero (stationary) laboratory mean velocity. Such discharges will also serve as velocity references for laser-induced fluorescence (LIF) based measurements of velocity (energy) distributions during thruster characterization. In this paper, the progress on developing this reference source is updated, including absorption measurements to characterize the ground state Bi density. The selection of suitable LIF candidate transitions is revisited, discussing selection criteria such as accessibility, signal strength, and availability of data for modeling hyperfine structure. A new opportunity to probe the BiII 680.9 nm transition based on recently introduced diode lasers is presented; this transition is seen to be very strong in emission and the LIF can be detected in non-resonant fluorescence. Transition lineshapes pertinent to this analysis will be modeled in terms of hyperfine splitting and broadening mechanisms. Recent progress in augmenting a laboratory SPT thruster to operate on a mixture of argon and bismuth will also be described.

Nomenclature

A	= magnetic moment hyperfine splitting parameter
B	= quadrupole moment hyperfine splitting parameter
ΔE	= energy shift due to hyperfine splitting by nuclear spin
E	= energy between two electronic states
F	= total atomic angular momentum quantum number, including nuclear spin
I	= nuclear spin quantum number
J	= total atomic angular momentum quantum number, excluding nuclear spin
j	= single electron angular momentum quantum number
L	= total orbital angular momentum quantum number
$n-L$	= species number density times absorption path length
λ, ν	= wavelength or frequency of light
n	= number density
S	= total electron spin angular momentum quantum number

* Research Assistant, Mechanical Engineering Department, scharfe@stanford.edu.

† Professor, Mechanical Engineering Department, cap@stanford.edu.

T = kinetic temperature
 u = bulk velocity (in direction of incoming laser beam)
 ν_0 = linecenter frequency

I. Introduction

Achieving the goal of faster missions to the outer planets requires significant improvements in the areas of spacecraft mass, efficiency, and flight time. The increase in velocity-increment required to significantly reduce the time of flight requires that either the propellant mass or the specific impulse (Isp) of the thruster be increased. Due to the dramatic cost increase associated with initially launching a larger-mass chemical rocket into Earth orbit, the method of choice for faster missions will lean toward high-Isp electric propulsion systems, like those flown on Deep Space I. However, state-of-the-art electric propulsion systems are still lacking in the efficiency and power handling required to effectively reduce flight time. Higher power Nuclear-Electric Propulsion (NEP) missions to the outer planets require a thruster capable of handling hundreds of kilowatts, while present ion engine technology is limited in power to less than 10 kW.

In order to accommodate the requirements of future NEP missions, a bismuth-fueled two-stage Hall Thruster with Anode Layer (TAL) was selected as an option for further development[‡]. The proposed thruster would build on the TAL 160 and TAL 200 thrusters developed to operate on storable metal vapor propellants by TsNIIMASH in Russia. A bismuth-fed Hall thruster offers significant advantages over ion thrusters; current TAL thrusters have been demonstrated to perform at 25-140 kW and have the potential to scale up to greater than 500 kW for future very high power NEP systems. Bismuth also offers several advantages over the xenon propellant used in current ion thrusters. Bismuth has a larger atomic mass, which serves to increase the thrust per particle for a rocket with a given Isp. Additionally, bismuth is condensable at room temperature, which allows for simpler testing on the ground in existing facilities as well as reduced spacecraft tankage fraction. Further, the ionization potential of bismuth is only 7.3 eV, compared to 12.1 eV for xenon, so that the propellant is more easily ionized and the thruster will have higher efficiency. Bismuth is also significantly less expensive and more readily available than is xenon.¹

As the Bi-fed Hall thruster is developed, there will be a need for precise optimization of geometry and operating conditions, as well as accurate predictions of the potential for spacecraft contamination. This process will be contingent upon a characterization of the internal and near-field neutral bismuth (BiI) and bismuth ion (BiII) energy distribution, velocity field, and particle flux. A combination of laser-induced fluorescence (LIF) and absorption spectroscopy will be used to perform a portion of the necessary diagnostics.

It is expected that LIF will be used to probe excited states in the BiI and BiII atomic and ionic particle stream to deduce the three-dimensional (3D) velocity (energy) distribution. While several electronic transitions of neutral and ionized bismuth are accessible with laboratory-laser systems (e.g., Ti-Sapphire or Ring-Dye lasers), they are not easily accessed with more compact laser sources that are more conveniently used in ground-test facilities suitable for thruster performance studies. While the least costly and most readily available portable diode laser would be the New Focus brand Vortex line of lasers, these lasers have a limited tuning range of roughly 0.2 nm in the IR and cannot capture certain transitions of the bismuth ion due to the wide hyperfine splitting of this species and the Doppler shift corresponding to the 70 km/s exhaust velocity expected for a two-stage Bi thruster. Therefore, selections for the ions will be designed to make use of the New Focus brand Velocity line of diode lasers, which have a broader tuning range. The selection of the transitions expected to be most useful in LIF analysis of the ions will be discussed in this work; selections have been modified since those previously presented^{2,3} to utilize more desirable transitions with a newly available Velocity laser. Additionally, these transitions will be modeled in terms of hyperfine splitting and broadening mechanisms; basic Doppler broadened (Gaussian) profiles will be modified to account for the more irregular velocity distribution predicted by a 2-D hybrid Hall thruster simulation developed at Stanford.

In addition to measurements of particle velocity, measurements of the number density of exhaust particles will be required for determining total particle fluxes. One possible option for ground state BiI number density will be the use of atomic resonance absorption spectroscopy of the 306.772 nm ($6p^3 \ ^4S_{3/2} - 7s \ ^4P_{1/2}$) transition (vacuum wavelength: 306.86 nm). For BiII, a transition with the ground state as the lower state is located at 143.68 nm ($6p^2 \ ^3P_0 - 7s \ ^3P_1$), which poses some difficulty as it is in the far vacuum-ultra-violet range.

Recent work has focused on the development of a means to measure features of interest in the bismuth spectrum prior to testing with a bismuth-fed thruster. A bismuth microwave discharge was described previously, but presented

[‡] See, for example: http://www.aviationnow.com/content/ncof/ncf_n84.htm and press release: <http://quest.arc.nasa.gov/aero/news/08-30-02.txt>.

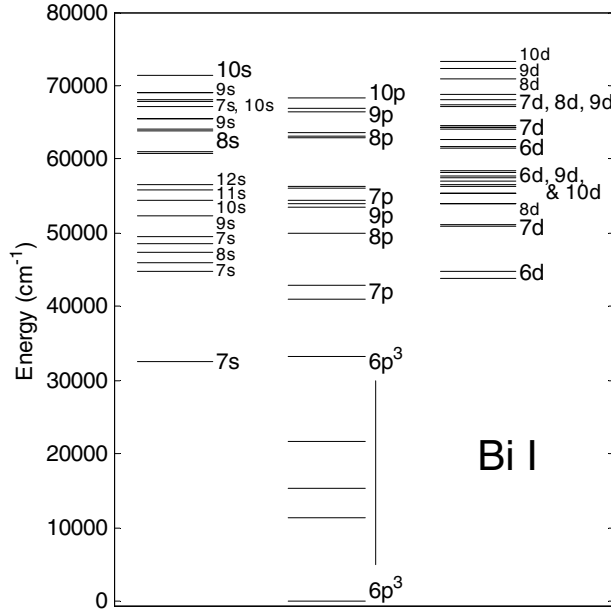


Figure 1. Overview of the energy levels of Bi I.

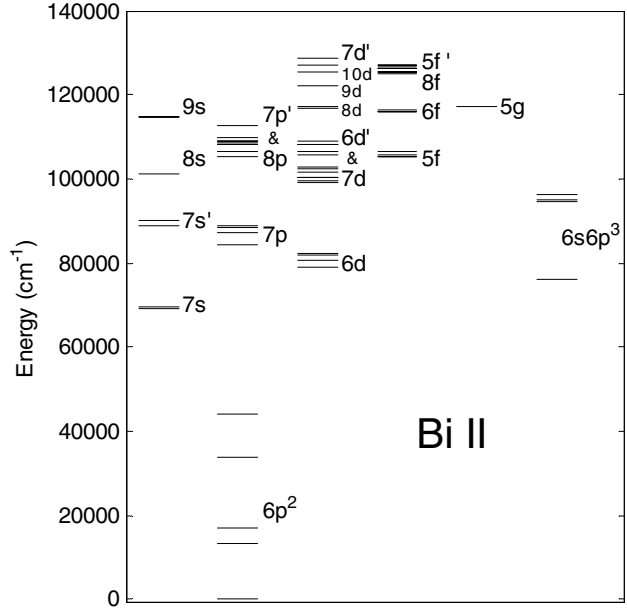


Figure 2. Overview of the energy levels of Bi II.

several difficulties.² For the present work, a bismuth heat pipe apparatus has been developed; this device will be discussed and measurements of the Bi spectrum recorded in absorption and emission spectroscopy will be presented. In addition to further modification and measurement on the heat pipe, several laboratory Hall thrusters are being modified to run on bismuth propellant for future analysis.

Various bismuth transitions as well as some preliminary measurements have been presented previously^{2,3}. This paper will summarize the basis of analysis of the bismuth spectrum, revise the line selections for future thruster measurements, and present refined measurements of the bismuth spectrum.

II. Transition Analysis

In order to make spectroscopic measurements and perform the subsequent analysis, the structure of each transition must be understood. To begin this discussion for bismuth, some general spectroscopy can first be reviewed. For any element, a Grotrian energy level diagram, like those for Bi I and Bi II shown in Figs. 1 and 2 above,^{4,5,6} can be constructed to indicate the allowed electronic energy levels. In the diagrams below, the configuration of the outermost electron is shown next to each energetic state. The energy difference between the states of an electronic transition defines the wavelength of emitted (or absorbed) light according to:

$$\lambda = \frac{hc}{E}. \quad (1)$$

Here, λ is the wavelength of light, h is Planck's constant, c is the speed of light, and E is the energy difference between two states (the energy of the emitted photon). However, each electronic state is further split due to the effects of nuclear spin and different isotopic masses. For bismuth, only one isotope need be considered, so the only splitting effects will be those due to the nuclear spin, I , which is $9/2$ for the case of bismuth⁵. This splitting is defined by energy shifts, ΔE , given by^{5,6,7}:

$$\Delta E = \frac{1}{2} AC + B \frac{3C(C+1) - 4I(I+1)J(J+1)}{8I(2I-1)J(2J-1)}, \quad (2)$$

where A and B are hyperfine splitting parameters for a given electronic state, and:

$$C = F(F+1) - I(I+1) - J(J+1). \quad (3)$$

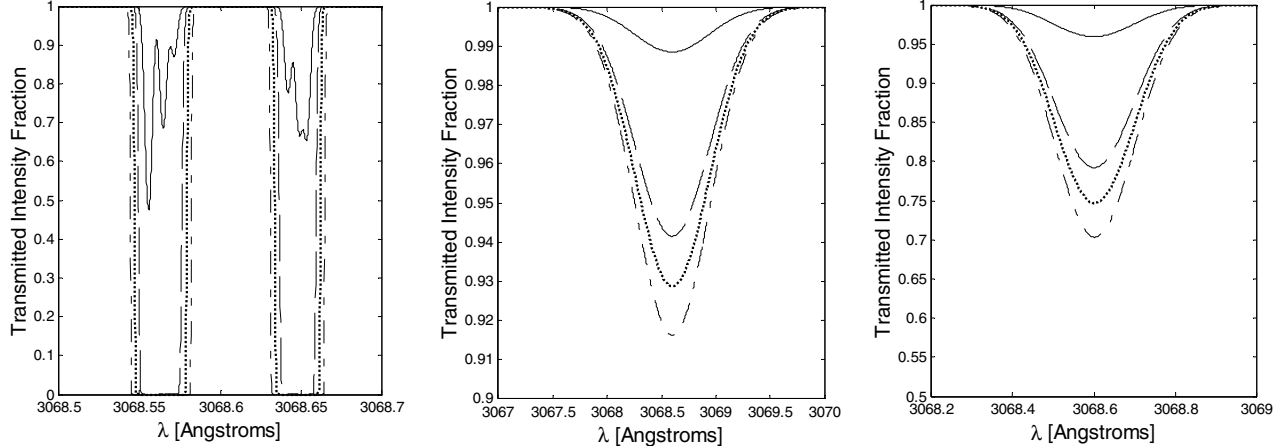


Figure 3. Simulated absorption profiles for resonance transition of BiI with 1000 K Doppler broadening. From left to right: true absorption profile, profile corresponding to 0.8 Angstrom instrument resolution, and profile corresponding to 0.2 Angstrom instrument resolution. In all plots: a solid line corresponds to $n\text{-}L$ product of $1 \times 10^{12} \text{ cm}^{-2}$, dashed line is $1 \times 10^{14} \text{ cm}^{-2}$, dotted line is $1 \times 10^{16} \text{ cm}^{-2}$, and dash-dotted line is $5 \times 10^{18} \text{ cm}^{-2}$.

F is the angular momentum including nuclear spin and can take on multiple values according to:

$$F = J + I, J + I - 1, \dots, |J - I|, \quad (4)$$

where J is the total angular momentum (neglecting nuclear spin) for the electronic state considered. To predict the splitting of an electronic transition, the selection rule for transitions between the F -states of upper and lower electronic energy levels is:

$$\Delta F = 0, \pm 1, \quad (5)$$

but with $F = 0$ to $F = 0$ forbidden. Further, the relative intensity of each hyperfine-split transition component is determined by the so-called “sum rules” which relate the total intensity of lines going to and from a given F -state to the degeneracy of that state.^{7,8,9}

When measured in the laboratory, transitions will typically be broadened. Typically, Doppler (assuming a Gaussian velocity distribution) and Lorentzian broadening mechanisms are examined, and the effects of each are convolved to produce a Voigt profile for a given transition.

Using these models, predicted absorption profiles can be produced for the 307 nm resonance transition of BiI, taking into account hyperfine splitting, broadening mechanisms, and approximating the instrument response with a Gaussian curve. An example of such a plot is shown in Fig. 3 above for a variety of $n\text{-}L$ products (BiI number density times absorption path length).

Simple Gaussian and Lorentzian broadening, however, is not expected to hold for the ions in the Hall thruster plume as their velocity distribution is not expected to conform to thermal equilibrium. A more accurate model for ion lineshape profiles will be discussed here.

III. Candidate Transition Selection

Previously,^{2,3} several candidate Bi transitions were selected for analysis and discussed. The transition selected for ground state BiI number density determination by atomic resonance absorption spectroscopy was the line at vacuum wavelength 306.86nm ($6p^3 \text{ } ^4S_{3/2} - 7s \text{ } ^4P_{1/2}$). Candidate transitions for velocity determination via LIF analysis of ions and neutrals were originally chosen based, in part, on accessibility to the New Focus Vortex line of lasers. The New Focus TLB-6000 Vortex series lasers can be tuned at the factory to specific wavelengths within the approximate ranges of 765-788 nm and 795-853 nm. Therefore, the 784.033 and 854.454 nm lines of BiI and the 796.5 and 853.2 nm (previously labeled 854.3 nm²) lines of BiII were selected at that time (Wavelengths here are measured in air, as listed by NIST;¹⁰ vacuum values are 784.25, 854.7, 796.7, and 853.4 nm, respectively).

The nature of the Bi spectrum, and the potentially high exhaust velocity of a two-stage Bi Hall thruster (estimated at 70 km/s), poses some additional difficulty in performing future LIF measurements, especially for the bismuth ion. While the Vortex lasers discussed above can be configured for a wide range of specific wavelengths at the factory, once in the laboratory each laser can only scan a range of 60-80 GHz (or roughly a maximum of 0.2 nm near 800 nm) about the factory-set central wavelength. It is noted here that the tentative LIF setup would require a single laser beam to be split to probe both the radial and axial velocities in the thruster plume simultaneously. The Doppler shift in transition frequency, $\delta\nu$, due to a mean velocity component, u , in the direction of the incoming laser beam, is given by:

$$\delta\nu = \nu_0 \frac{u}{c}, \quad (6)$$

where ν_0 is the unshifted linecenter frequency and c is the speed of light. For an axial velocity component of 70 km/s probed by a laser of roughly 800 nm, this corresponds to a shift of 87 GHz, or roughly 0.2 nm. Based on the Doppler shift alone, it would be quite difficult to probe the fast axial velocity and the slower moving radial velocity of a two-stage thruster with a single Vortex laser. Further complicating matters, the 796 nm line of BiII has a predicted hyperfine width of 0.18 nm, and the BiII line at 853 nm has a width of 0.11 nm,² making the task of scanning the entire shifted lineshape of a BiII transition for a variety of velocities up to 70 km/s impossible with a single Vortex model laser.

Therefore, the next option is to use the New Focus brand Velocity line of lasers for measurement of ion velocities. Previously,³ lasers of interest included the Velocity TLB-6312 which can scan from 765-781 nm, and the Velocity TLB-6316 which can scan 838-853 nm. At the time, these were the only Velocity lasers that could hit BiII lines, and therefore selection was limited to the only BiII lines within these ranges: those at wavelengths in air of 775.0 nm and 838.8 nm, as listed by NIST (these lines are at 775.2 and 839.0 nm, respectively, in vacuum).³ However, New Focus has recently introduced several new Velocity laser models that can access several additional BiII lines. This has opened up the selection significantly and allowed for greater choice in the selection of a transition for LIF analysis. Specifically, the TLB-6309, which can scan 680-690 nm has been selected to probe the NIST-listed 680.86 nm line of BiII. Dolk et al., place this line at 680.91 nm with designation $6p7s(1/2,1/2)_1 - 6p7p(1/2,1/2)_1$.^{5,11}

The selection of the 680.9 nm transition provides several advantages. Aside from being accessible to a New Focus Velocity laser, the 680.9 nm line is a relatively strong transition according to NIST data;¹⁰ in fact, it is the strongest BiII line in the 600-900 nm

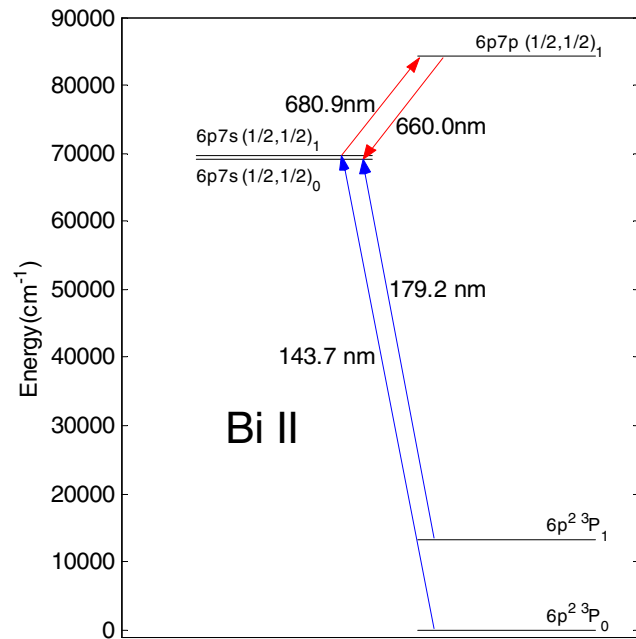


Figure 4. Partial Grotrian diagram for BiII indicating the transitions of interest for LIF analysis.

Table 1. Transitions corresponding to the 143.7, 179.2, 660.0, and 680.9nm lines of BiII, using the energy level data and transition assignments from Dolk et al. and Crawford et al.^{4,5,11} Starred transitions indicate wavelength measured in vacuum. Note that 1 mK = 10⁻³ cm⁻¹.

Wavelength in Air [nm]	Lower Level				Upper Level			
	Energy [cm ⁻¹]	Designation	A [mK]	B [mK]	Energy [cm ⁻¹]	Designation	A [mK]	B [mK]
143.68*	0.000	6p ² 3P ₀	--	--	69598.475	6p7s(1/2,1/2) ₁	390.7	3
179.18*	13325.401	6p ² 3P ₁	-82.9	-16.5	69133.891	6p7s(1/2,1/2) ₀	--	--
660.03	69133.891	6p7s(1/2,1/2) ₀	--	--	84280.446	6p7p(1/2,1/2) ₁	269.25	1
680.91	69598.475	6p7s(1/2,1/2) ₁	390.7	3	84280.446	6p7p(1/2,1/2) ₁	269.25	1

region that is most useful for this work. Additionally, an analysis of the energy level structure of BiII, depicted in Fig. 4, shows that the 680.9 nm transition shares an upper state with the 660.0 nm transition, which may be useful for non-resonant LIF collection. The 660.0 nm transition (configuration: $6p7s(1/2,1/2)_0 - 6p7p(1/2,1/2)_1$)^{5,11} is the second strongest BiII line listed by NIST in the region of interest.¹⁰ High intensity of both the probed transition and the collected transition should help to maximize signal strength in thruster measurements. Further, Dolk et al.⁵ state that the “connection between the two lowest levels...of the ground configuration [of BiII] and the excited configurations is established by the lines at 1436 Angstroms and 1791 Angstroms.” A further analysis of the energy level structure of BiII, illustrated in Fig. 4 and Table 1, shows that these ultra-violet transitions, which provide a bottleneck for the excitation and de-excitation of BiII states, connect the ground configurations of BiII with the lower levels of the 680.9 nm and 660.0 nm transitions. Therefore, the lower level of the 680.9 nm transition should be well populated, further maximizing the number of ions that can be excited by a laser at this wavelength and improving LIF signal strength. The hyperfine split profiles of both of these transitions are shown in Fig. 5 below.

Unfortunately, there are no BiI lines¹⁰ that can be probed using the Velocity laser systems that may be useful in ion measurements. However, neutral Bi particles are not expected to be accelerated to the same high velocities as the ions. Additionally, the hyperfine splitting of BiI is relatively narrow when compared with that of the ion lines: the BiI line at 784 nm is predicted to have a hyperfine split width of only 0.06 nm, and the line at 854 nm is expected to be split to roughly 0.02 nm wide.² These lines, therefore, may still be accessible to the less expensive Vortex class lasers from New Focus and their analysis is unchanged from that presented previously.²

IV. Revised Lineshape Model

Previously,² lineshapes were modeled assuming a shifted-Gaussian velocity distribution for ions and neutrals corresponding to various kinetic temperatures for the particles. However, the positioning and distribution of the ionization zone relative to the potential drop in the thruster, combined with collisions between fast-moving ions and slow neutrals, can result in significant distortion to the velocity distribution – for ions, for example, this can result in a group of fast moving particles and a smaller group of slow moving particles in a clearly non-Maxwellian velocity distribution. Simulations have shown that rather than a thermal profile, the ion velocity distribution function would be based primarily on the distribution of the ionization zone relative to the spatially varying thruster potential. An example of this effect is illustrated in Fig. 6 on the following page for the 680.9 and 660.0 nm transitions. The ion velocity distribution used here is taken from the exit plane in a 2-D hybrid Hall thruster simulation developed at Stanford University. Note that the broadened profiles of each line clearly show the result of the hyperfine structure – these profiles are in the range of 0.15-0.25 nm wide and should be resolvable with a tunable laser source. Typical

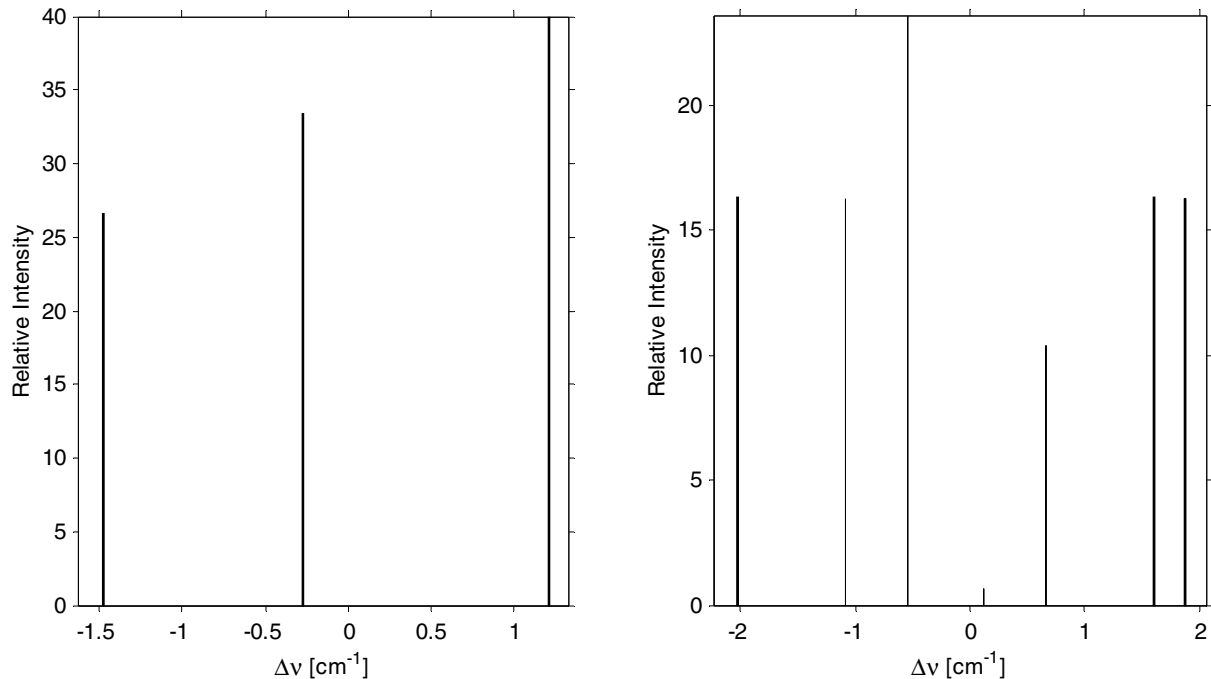


Figure 5. Hyperfine splitting profiles of BiII transitions. From left to right: 660.0 nm transition and 680.9 nm transition.

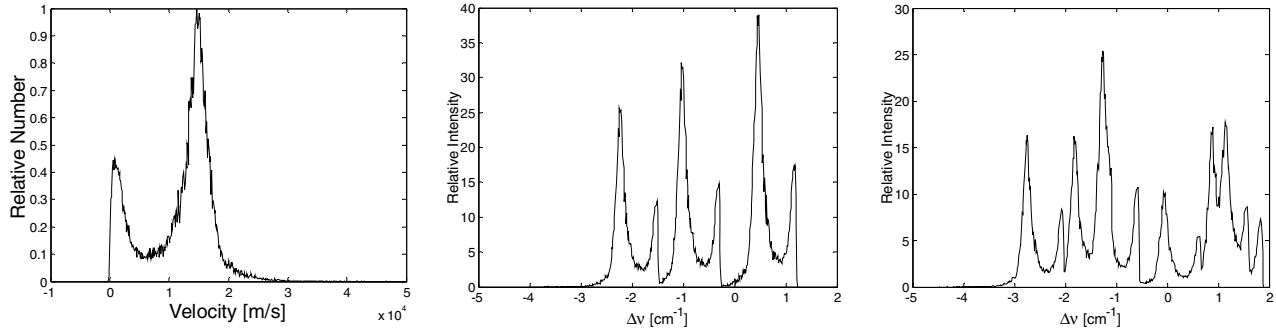


Figure 6. Simulated velocity distribution and resulting Doppler broadening of BiII lines. From left to right: Velocity distribution calculated at exit plane of simulated thruster, broadening of 660.0nm line, and broadening of 680.9nm line of BiII.

thruster measurements on xenon do not generally show the effects of its comparatively narrow hyperfine splitting.⁷ Additionally, the width of these lines evidences the need for lineshape models before attempting diagnostic measurements, as discussed above with regard to selecting appropriate New Focus lasers.

V. Measurements of Bi Spectrum

A bismuth heat pipe apparatus, based on the design of Cappelli, et. al.^{12,13} and illustrated in Fig. 7 below, has been developed in order to measure and further analyze the Bi spectrum before putting the diagnostics to use on an actual thruster. The apparatus consists of an electrically heated metal mesh inside a small vacuum chamber. Bismuth is placed onto the center of the mesh, and the outer edges of the mesh are cooled so that the vaporized bismuth will condense out and wick back toward the hot center. Argon is pumped into the chamber to help contain the bismuth in the cavity and prevent it from plating out onto the walls and windows. Additionally, a pair of electrodes inside the chamber is used to generate a hollow cathode discharge that produces light-emitting Bi plasma. The electrodes are typically run at 600 V with current on the order of several milliamps. A deuterium lamp outside the chamber is used as a broadband light source for absorption analysis near the BiI resonance transition. A thermocouple between the electrical heater and the heat pipe mesh is used to estimate the temperature (and therefore the vapor pressure) of the Bi inside the chamber. Data was recorded using a ½ m monochromator and a Hamamatsu R928 photomultiplier tube (PMT). The exit and entrance slits of the monochromator were held at 10 μm for absorption scans, and from 10-40 μm for emission measurements. The signal from the PMT was passed to a Stanford Research SR850 Lock-in Amplifier.

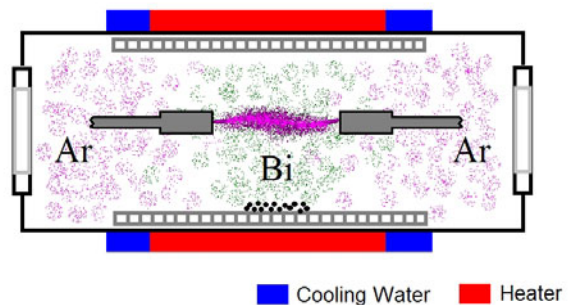
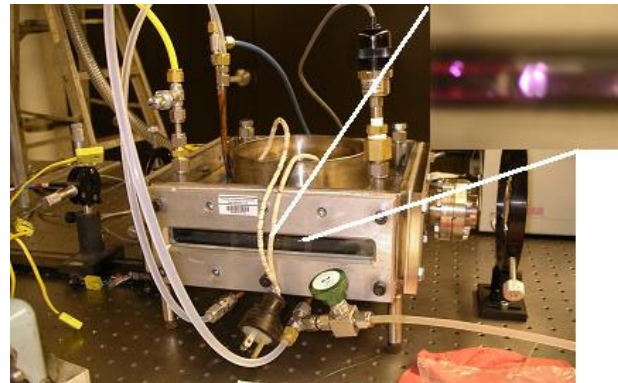


Figure 7. Bismuth Heat Pipe apparatus.

Thus far, the heat pipe has been used to successfully record both absorption and emission from the 307 nm resonance transition of neutral bismuth. Representative scans of emission and absorption are shown in Fig. 8 on the following page. It is noteworthy that the corresponding bismuth partial pressure estimated from the absorption scan is close to the equilibrium pressure for bismuth at a temperature of 800°C (discussed below), within experimental uncertainty of the cell operating temperature of 850°C. Note that as the chamber is cooled, the absorption disappears because the vapor pressure of the bismuth is decreasing; this verifies that the line observed is indeed bismuth. Similar results were seen

for emission scans. However, after heating the chamber for an extended period and then cooling it, the bismuth line would still appear in the emitted light, indicating that perhaps an amount of bismuth had plated out onto the electrodes and was being re-vaporized without the need for the electrical heaters.

A simple analysis of the peak absorbed fraction of light can be used to estimate the $n-L$ product discussed earlier in this paper. Based on the width of the absorption profiles, and analysis for various instrument resolutions as illustrated in Fig. 3, it is estimated that the instrument resolution for these trials corresponds to roughly 0.8 Angstroms in modeled profiles. Comparing to the data in Fig. 3, and estimating an absorption path length of 10 cm inside the cell, the peak absorption fraction at each temperature can be used to estimate the vapor pressure, and therefore the temperature, of the bismuth in the cell. For example, at 850°C, the average absorbed fraction was 7%. This would correspond to an $n-L$ product of roughly $1 \times 10^{16} \text{ cm}^{-2}$, and therefore a number density of $1 \times 10^{15} \text{ cm}^{-3}$. At roughly 1000 K, this would correspond to a bismuth pressure on the order of 100 millitorr; this vapor pressure corresponds to a bismuth temperature closer to 800°C, providing an estimate of the temperature drop between the thermocouple and the inside of the heated mesh. However, a more precise analysis, requiring iteration of the temperature (used in Doppler broadening of the transition and calculating pressure from number density), a more accurate determination of the instrument resolution (FWHM of Gaussian response curve), and an averaging of multiple measurements to reduce signal noise, would be necessary to make calculations beyond order-of-magnitude. What is more important here is that as the temperature was reduced, the corresponding drop in bismuth number density was observable in a qualitative sense in the absorption profiles. This type of relative analysis will be important in analyzing a thruster, where precise species temperatures for Doppler broadened transitions may not be instantaneously available for an exact analysis. The variation in the absorption with temperature is illustrated in Fig. 8. As expected, there is a strong dependence in the absorption with temperature, since the vapor pressure of bismuth varies exponentially with temperature.

Although the 307 nm line was observed consistently in both absorption and emission, there is some uncertainty in the measurement of the candidate transitions for BiII due to interference from nearby Argon transitions. Nonetheless, it does appear that BiII lines are being observed in emission. As shown in Fig. 9 on the following page, emission measurements were recorded near 520 nm to attempt to measure the BiII line at 520.9 nm – the strongest bismuth ion line in the visible/near IR region. Though this line is relatively weak next to the strong Argon lines that appear near it (and can be used to provide an assurance of instrument calibration), it was measured consistently. Further, emission measurements were recorded near 660 nm to attempt to measure the candidate BiII line for non-resonant LIF collection. However, the 660.0 nm BiII line is masked by the ArI line at 660.48 nm. In the future, however, this interference should not be a problem in LIF analysis as the 680.9 nm laser beam will be chopped for phase-sensitive detection of the non-resonant BiII fluorescence; measurement of 660.0 nm light at the chopped frequency will exclude any emission from the argon lines in this region. Finally, measurements were recorded near 680 nm to record the 680.9 nm BiII transition. It appears that this transition was observed successfully, and it is located near the slightly stronger ArI line at 682.7 nm. A hint of the ArI line at 681.8 nm may also be visible here. It should be noted that there is an ArII line listed in NIST at 680.85 nm; however, it is not

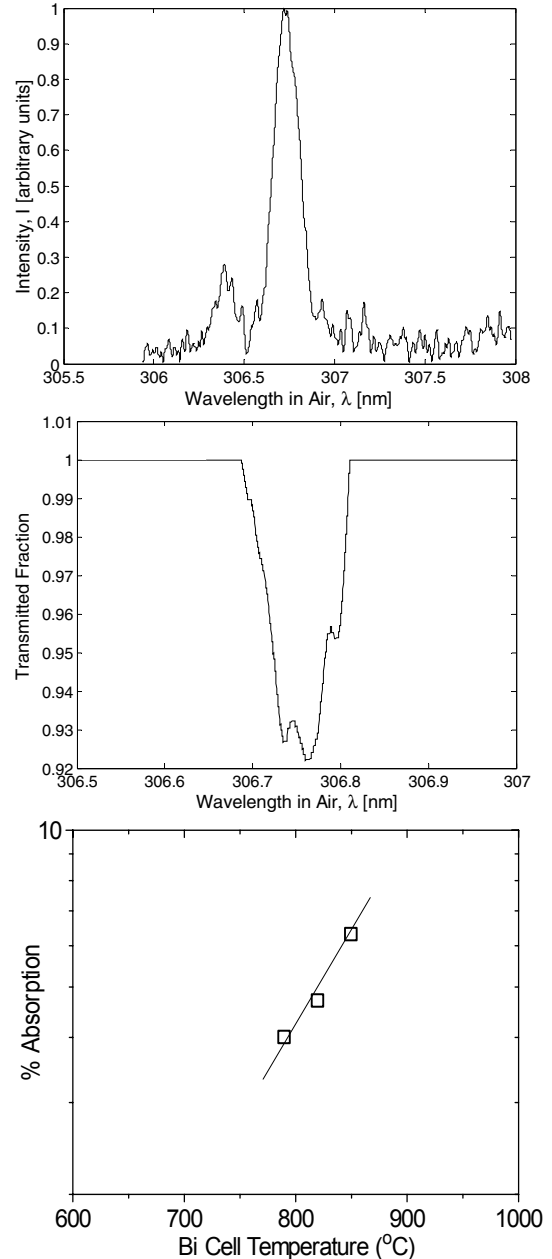


Figure 8. Measurements of the BiII resonance line in the heat pipe chamber. From top to bottom: emission, absorption at 850°C, and absorption versus cell temperature.

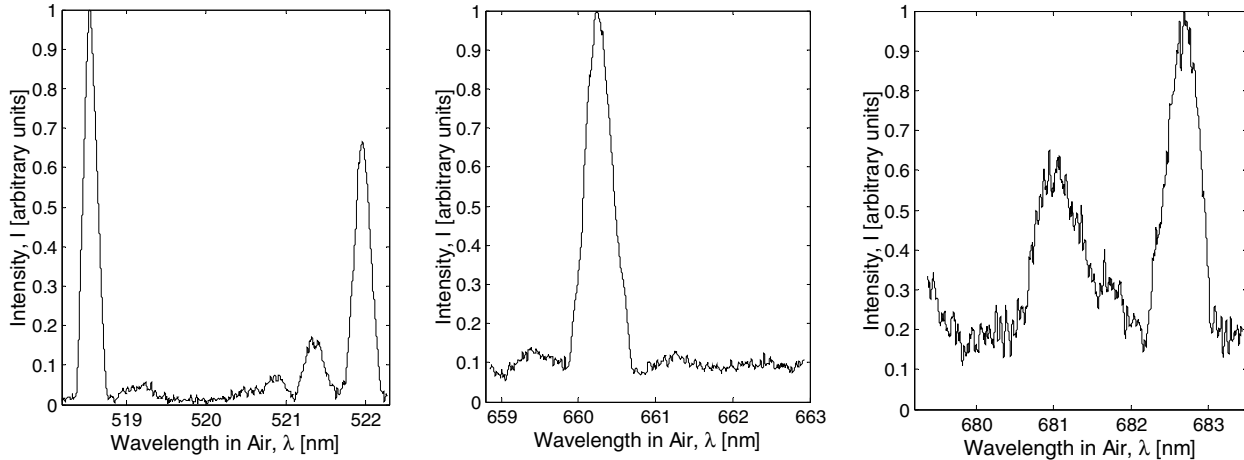


Figure 9. Emission measurements of various Bi II lines. On the left, measurement of BiII 520.92 nm line surrounded by ArI 518.77 nm, ArI 522.127 nm, and what may be ArII 521.68 nm. In the center is data near the BiII 660.0 nm line; it is masked by ArI 660.48 nm. On the right is the BiII 680.86 nm line near ArI 682.7 nm; ArI 681.82 nm may also be visible in the trace.

assigned a strength and should be much weaker than any bismuth ion lines due to argon's significantly higher ionization energy. Therefore, it is likely that this measurement actually shows the BiII line that will be probed in LIF. Before testing with a laser, future experiments will focus on verifying that these lines are indeed bismuth, by, for example, altering the heat pipe temperature and assuring that the signal drops in proportion with the bismuth vapor pressure.

On a separate front, the development of a test thruster article for generating energetic BiII ions continues. An SPT thruster is being modified with a bismuth propellant feed system to generate a high velocity bismuth plasma (see Fig. 10). The existing thruster has been fitted with an electrically heated bismuth vaporizer cell coupled to a modified anode to inject bismuth into the channel (see inset to Fig. 10). At present, the anode distributor is not separately heated, but relies on heating by energetic electrons in the mixed argon-Bi plasma. Argon, which is used as the cathode gas and to start the discharge, is injected in a second distributor located upstream of the Bi distributor/anode. As of the writing of this paper, a stable discharge in this configuration has not yet been sustained.

VI. Conclusion

As work continues on this project, advancement of the diagnostics will be continued by increased modification to the heat pipe cavity to provide a more controllable bismuth vapor source. The geometry and operating conditions of the electrodes will be redesigned to produce a stronger discharge that should generate a higher ionization fraction and greater electronic excitation; the aim is to produce a better tool for measuring excited states of BiI and BiII and analyzing the candidate transitions with improved signal strength and consistency. The simulations of LIF spectral lineshapes have been extended, and although a number of suitable candidate transitions accessible with commonly available diode lasers have been identified, the recent introduction of a diode laser that spans the 680-690 nm range has created a new option – the probing of a strong transition in BiII at 680.9 nm. Finally, the fabrication has been completed for an SPT thruster that will operate on mixtures of argon and bismuth for further refinement of diagnostic techniques.

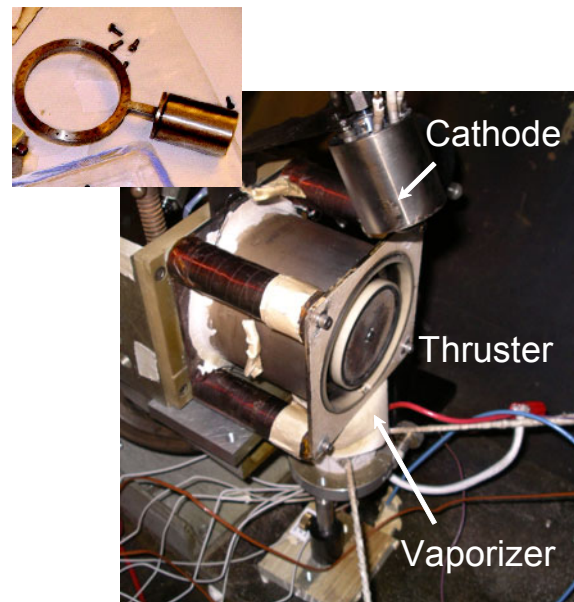


Figure 10. Photograph of the modified SPT thruster for Bi/argon operation. Inset shows the details of the vaporizer/distributor.

Acknowledgments

The research was conducted under a contract with the National Aeronautics and Space Administration. The authors would like to thank John Warren in the Prometheus Advanced Systems and Technology Office for support of this work. Partial support for D. Scharfe is provided through a fellowship from the Department of Defense/ASEE.

References

- ¹Tverdokhlebov, S., Semenkin, A., and Polk, J., "Bismuth Propellant Option for Very High Power TAL Thruster," *40th AIAA Aerospace Sciences Meeting & Exhibit*, AIAA, 14-17 January 2002.
- ²Scharfe, D.B., and Cappelli, M.A., "Optical Diagnostic Options for Bismuth Hall Thrusters," AIAA-2004-3946, *40th AIAA/ASME/ASEE Joint Propulsion Conference*, AIAA, 11-14 July 2004.
- ³Scharfe, D.B., and Cappelli, M.A., "Spectroscopic Measurements of Bismuth for Optical Diagnostics," AIAA-2005-4230, *41st AIAA/ASME/SAE/ASEE Joint Propulsion Conference*, AIAA, 10-13 July 2005.
- ⁴Moore, C.E., *Atomic Energy Levels as Derived From the Analyses of Optical Spectra*, Volume III, National Bureau of Standards, Circular 467, U.S. Government Printing Office, Washington, D.C., 1958, May 1, 1958, pp219-222.
- ⁵Dolk, L., Litzen, U., and Wahlgren, G.M., "The Laboratory Analysis of Bi II and its Application to the Bi-rich HgMn Star HR 7775," *Astronomy & Astrophysics* 388, 2002, pp. 692-703.
- ⁶George, S., Munsee, J.H. and Vergès, J., "Hyperfine-structure Measurements in Bismuth Using a Fourier-transform Spectrometer" *J. Opt. Soc. Am. B*/Vol. 2, No. 8, August 1985, pp. 1258-1263.
- ⁷Cedolin, R.J., *Laser-Induced Fluorescence Diagnostics of Xenon Plasmas*, Report No. TSD-105, Ph.D. Dissertation, High Temperature Gasdynamics Laboratory, Mechanical Engineering Dept., Stanford University, Stanford, CA, June 1997, p. 56.
- ⁸Sobelman, I.I., *Atomic Spectra and Radiative Transitions*, 2nd ed., Springer-Verlag, New York, 1992, p. 170.
- ⁹Kuhn, H.G., F.R.S., *Atomic Spectra*, Academic Press, New York, 1969, p.191.
- ¹⁰NIST Atomic Spectra Database Lines Form, http://physics.nist.gov/cgi-bin/AtData/lines_form.
- ¹¹Crawford, M.F., and McLay, A.B., "Spark Spectra of Bismuth, Bi III and Bi II," *Proceedings of the Royal Society of London*, Series A, Vol. 143, No. 850, Feb. 1, 1934, pp. 540-557.
- ¹²Cappelli, M.A., M.A.Sc. Thesis, U. Toronto, Institute for Aerospace Studies (1983).
- ¹³Cappelli, M.A., Cardinal P.G., Herchen, H., and Measures, R.M., "Sodium atom distribution within a heat sandwich oven," *Rev. Sci. Instrum.* 56 (11), November 1985, pp. 2030-2037.